International Journal of Geography, Geology and Environment

P-ISSN: 2706-7483
E-ISSN: 2706-7491
IJGGE 2024; 6(1): 430-445
www.geojournal.net
Received: 12-03-2024
Accepted: 16-04-2024

Hanan Rasooli
[1] Department of Geography and Urban Planning, Faculty of Humanities and Social Sciences, University of Mazandaran, Babolsar, Iran
[2] Department of Geography, College of Education for Women, University of Basrah, Basrah, Iraq

Sedigheh Lotfi
Department of Geography and Urban Planning, Faculty of Humanities and Social Sciences, University of Mazandaran, Babolsar, Iran

Amer Nikpour
Department of Geography and Urban Planning, Faculty of Humanities and Social Sciences, University of Mazandaran, Babolsar, Iran

Corresponding Author:
Hanan Rasooli
[1] Department of Geography and Urban Planning, Faculty of Humanities and Social Sciences, University of Mazandaran, Babolsar, Iran
[2] Department of Geography, College of Education for Women, University of Basrah, Basrah, Iraq

Analyzing environmental and land use changes by combining remote sensing and geographic information system

Hanan Rasooli, Sedigheh Lotfi and Amer Nikpour

DOI: https://doi.org/10.22271/27067483.2024.v6.i1f.248

Abstract
Arid and semi-arid regions exhibit distinct spectrum features compared to other climatic regions. Hence, this work used remote sensing and geographical information system to identify environmental and land use alterations in the city of Basrah, located in southern Iraq. Various picture indices are employed. The analysis utilizes three mean Landsat photos from the years 2002, 2012, and 2022 to identify alterations in the environment and land utilization. This study suggests utilizing various indices to chart the alterations in the environment using Landsat 7 and 8. The mapping process would be facilitated by the cloud computing-based Google Earth Engine (GEE) platform, which efficiently manages images and processes spatiotemporal data on a large scale. Nevertheless, this platform necessitates the utilization of index formulae or combinations to facilitate the classification and enhance the precision in mapping the surface of the planet. The combination is made up of four indexes namely: vegetation index (NDVI), soil index (BSI), water index (NDWI), and buildings index (NDBI). In the change detection analysis, between 2012 and 2002, the vegetation cover had a serious degradation. The change detection results from BSI illustrate that the year of 2002 has the majority of bare soil rather than 2012 and 2022. According to the analysis, which was made on the Normalized Difference Moisture Index (NDMI) of Landsat (2012) image, the water level in the research area was increasing securely, while it was a decrease in 2002 compared to today. The process of urbanization is progressing as shows in the result of change detection analysis with the utilization of Normalized Difference Built-up Index (NDBI). The study investigates the changes in land use and land cover (LULC) patterns and its extent for the last twenty years using Maximum Likelihood Algorithm (MLA) and GIS technology. The maximum likelihood approach was used to classify the land use land cover (LULC) classes by using supervised classification technique.
Within the 2002 and 2022 interval, there was a huge decrease of the area of vegetative land coverage, which decreased from 20.21% to 2.79%. On the other hand, the area of barren land experiences a little decrease, which changes from 67.18% to 64.57%. In the meanwhile, with the analyzed land use and land cover (LULC) Classes water body and built-up area in the research area are growing, from 5.6618% to 13.31% and from 6.95% to 19.33% separately.
The results suggest that prioritizing and implementing integrated land management and land use planning within the research area is essential.

Keywords: NDVI, BSI, NDWI, NDBI, LULC change, Basrah, remote sensing, image indices, supervised classification

1. Introduction
In recent years, a variety of remote sensing techniques, such as aerial photography and satellite imaging, have come into common use for collecting data to map and monitor land use and land cover. Urban sprawl has caused urbanization rates and landscape changes to grow rapidly at metropolitan areas worldwide. These remote sensing data supply current information, as well as a synoptic view of landscape attributes and changes in metropolitan regions (Zha *et al*., 2003) [43].
Recently, remote sensing and GIS have been useful tools for studying various phenomena ranging from environmental impacts assessment and pollution monitoring using satellite images (Hadeel *et al*., 2011) [14]. Change Detection is the process of determining differences in the condition of an object or phenomenon by observing it at different times.

It's basically concentrating on mostly measuring temporal impacts by gathering some datasets collected at different intervals in succession. Describing land degradation it's like when people discuss about the loss in the quality or depletion of the potential or actual use of the spatial ecosystem, which was caused by the dynamic process, either naturally or man-made, is also referred to as land degradation. Change detection is often specified to the simultaneous acquisition of data sets needed to provide the analyst with the temporal dimension in the moiré. Although it can detect some changes between the sets, the change doesn't explain explicitly how long the change has elapsed.

Using spectral indices is an effective way to distinguish different types of land cover. Remote sensing has become a very powerful tool for detecting and mapping a wide range of characteristics on the Earth's surface. Typical applications include vegetation, soil, and water monitoring, characterization of developed regions, and so on. One of the most prevalent and widely used vegetation indexes, the Normalized Difference Vegetation Index (NDVI), is abbreviated as NDVI, to assess the vegainess, the fitness of vegetation, and the disparity of vegation content. This knowledge can be obtained through a comparison of the red (R) bands of the electromagnetic spectrum with the near-infrared (NIR) bands (Tucker, 1979) [38]. It involves various areas of research, such as the estimation of vegetation cover, the prediction of phenological changes, and the calculation of net primary production (Huang *et al*., 2014; Wu *et al*., 2008) [19, 40].

The BSI is part of the Near Infrared and Shortwave Infrared cartridge, which characterizes the nature of a soil and is used to classify areas with little or no vegetation. The BSI is calculated by subtracting the reflectance values of the two bands. The soil analysis, land use and land cover change detection, monitoring soil conditions, and monitoring land degradation (Nguyen *et al*., 2021; Zhu, Han, *et al*., 2021 water index is NDWI.) [27, 44].

To obtain water index, the near-infrared and shortwave infrared bands from the multispectral satellite or sensor are used to come up with this. This technique has been widely applied in many kinds of applications, such as water resources management, flood monitoring and coast line mapping. The NDBI is a well-known built-up index which acts as a tool in GIS. The calculation of this index would require the near-infrared and short wave infrared spectral bands to do the calculation. After getting the features, it has can be used to locate and map metropolitan areas and built-up. It has later widely exploited in both urban monitoring planners' use change and UHI.

The investigation of different LULC modifications has been of utmost significance in recent periods. It carries an immense impact, not only on surroundings, inhabitant species, and variety of life, but as well on human societies. The term of LULC alteration can be defined as the progress from a specific land fully of complexion to another. Consider an example, mutation of the semi-natural into agriculture tracts, or wet region to urban stretch.

It has been demonstrated by studies that changes in land use and land cover (LULC) are driven by a range of factors including population growth, urbanization, and economic development (Lambin *et al*., 2001) [23]. The increase in land conversion to agriculture means that there is serious deforestation and loss of natural habitat which, in consequence, has led to the decrease of biodiversity and disturbed ecological system (Foley *et al*., 2005) [10]. Urbanization, where the area of natural habitat are changed to build-up areas, causes depletion of ecosystems services and increasing environmental contamination (Seto *et al*., 2012) [34].

The land use and land cover (LULC) classification is executed through the remote sensing and GIS to recognize the changes and keep it under observation. It is a technique to distinguish the changes in land use and land cover and monitoring over the geographic area holding a grip on time interval of change. The changes in land use and land cover (LULC) have major impact in physical environment and human societies. The deforestation and changes in land use cause the climate change producing the carbon store in the atmosphere (Houghton, 2003) [17]. Also, the changes in land use and land cover (LULC) has many impact in local climate changes involve the changes involve the temperature and precipitation patterns. It also effect on the water quality and availability (Pielke *et al*., 2011) [30].

The changes in land use are mostly caused by the increase in population, expansion of agriculture, urbanization, growing needs for energy and food and shifts in lifestyles and socio-economic conditions. Therefore, Analysis of land use and land cover (LULC) change is a key source of data that support Decision Support Systems for policy makers (Tewabe and Fentahun, 2020) [36]. Alteration of land use and land cover (LULC) has been established as a major driver of environmental degradation and socio-economic instability (Lambin *et al*., 2001) [23]. Transformation of natural habitat into agricultural land, urbanization and infrastructure development resulted in depletion of biodiversity, soil erosion and harming quality of water (Geist & Lambin, 2002) [13]. Moreover, alteration of land use and land cover (LULC) is interrelated with increasing greenhouse gas emission which contributed for climate change (Fearnside, 2005) [9]. Indigenous populations frequently face dispossession, the disappearance of traditional livelihoods, and growing impoverishment from LULC change (Angelsen & Kaimovitz, 2001) [3]. Additionally, transforming LULC may help in exacerbating food insecurity. This is the case because the output of crops through soil degradation and reduced water availability decline (Schmidhuber & Tubiello, 2007) [33].

Various investigations have explored Land Use and Land Cover (LULC) dynamism in different parts of Iraq. These studies tried to inventory changes using Remote Sensing and GIS techniques via multitemporal and multispectral Satellite datasets e.g. Landsat, MODIS images collected in various periods of time. The results of these studies indicated the necessity of employing appropriate and sustainable Land Management techniques to mitigate the impacts of environmental degradation, and to ensure the eternal sustainability of Iraq's Natural resources.

With 30-pixel spatial resolution, the analysis is undertaken with Landsat 7 and 8 satellite images making use of "categorical" method employed by Google Earth Engine (GEE) mapping platform. The outcomes of these studies may be helpful to key information regarding the shifts and alterations in the Land Use and Land Cover (LULC) in Basrah city. The data accessed might be handily employed in supervising and appraising the world physiographic of Land Use. Additionally, such analyses throw considerable light on the need of Nature Resource Management (NRM) sustainability with regarding the government key interest at

separate regional scale and at national scale, while helping decision-maker groups, unintentional and intentional stakeholders, which the local group have in Basrah province.

2. Materials and Methods

2.1 Study area

Basrah City is situated in the southeast corner of Iraq approximately 420 km southeast of Baghdad, the capital of the Iraq. Basrah is located near to the Persian Gulf, at the point where the Shatt al-Arab River meets with the Gulf. This position makes the city very advantageous for trade and business. Basrah City covers an area of approximately 181 km and has a very large population. Basrah is one of the largest cities in Iraq.

Basrah City has a strong cultural heritage that was originated in the 7th century AD. At the time of the Abbasid Caliphate, Basrah City served as a major center for trade and business. It gained recognition for its lively markets, diverse culture, and notable architectural landmarks. Presently, the city accommodates numerous significant landmarks, such as the Basrah Museum, the Corniche, and the Old City, which exemplify its cultural and historical importance.

Basrah City encounters various environmental issues, such as air and water pollution, desertification, and the repercussions of climate change. The city's close proximity to the Persian Gulf renders it susceptible to the adverse effects of rising sea levels, saltwater intrusion, and coastal erosion. In addition, the city's swift process of becoming more urbanized and industrialized has resulted in a rise in air pollution, which presents health hazards to the population.

Geographically, Basrah city is situated. The astronomical position of the location is defined by its latitude, which falls between 30.20 and 30.50 degrees North, and its longitude, which falls between 47.25 and 47.55 degrees East. The elevation of the research region varies from -75 to 61 meters above the mean sea level, as shown in Figure 1.

Basrah City, situated in the southern region of Iraq, encounters a scorching desert climate, distinguished by exceedingly high temperatures and arid conditions during summers, and rather temperate winters. The summer season in Basrah, spanning from May to October, is characterized by scorching temperatures and arid conditions. During the peak summer months of July and August, the average high temperature can surpass 40 °C (104 °F), and it is not unusual for temperatures to climb as high as 50 °C (122 °F). The summer heat in the city is severe because of its proximity to the desert and the Persian Gulf. In the summer, the nights are warm as well, with average low temperatures usually exceeding 30 °C (86 °F).

The winter season, spanning from November to April, exhibits a comparatively temperate and agreeable climate. The mean maximum temperatures throughout the winter months fluctuate between 20 °C (68°F) and 25 °C (77°F), while the mean minimum temperatures can descend to approximately 10 °C (50°F).

Precipitation in Basrah is infrequent and irregularly apportioned throughout the year. The city has an annual rainfall of less than 100 mm, with the majority of precipitation occurring from December to March. Despite this, even during these months, rainfall is infrequent and does not provide a substantial addition to the city's water resources.

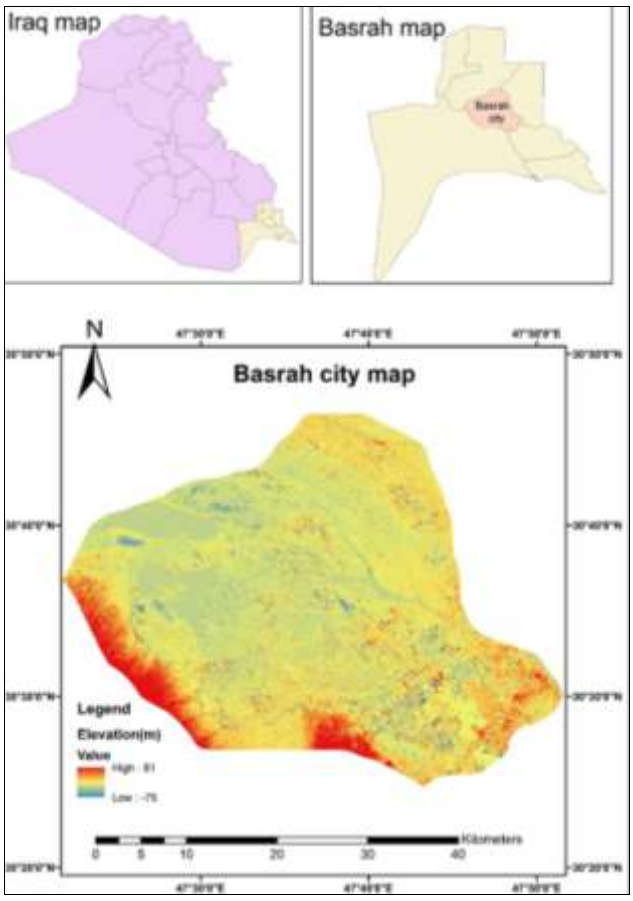

Fig 1: Study area map of Basrah City

Basrah City in summer is so hot and rainless have plentiful effects on the availability and quality of water in the city. The city is mainly supplied water from Shatt al-Arab River. But the river is easy to be polluted, the intruded salt water from the Arab Gulf and damaged by constructions of dams in the upper rivers.

Situated in southern Iraq, the city of Basrah has notable geological features that have been studied extensively. To begin, the area lies in the Mesopotamian Fore deep, a significant tectonic depression that has developed due to the collision between the Arabian and Eurasian plates (Jassim and Goff, 2006) [21]. Moreover, the most characteristic sediments of the area are Quaternary alluvial and deltaic sediments, which were deposited by the Tigris and Euphrates rivers (Al-Jiburi and Al-Basrawi, 2015) [2]. Moreover, the geological pattern of Basrah is affected by numerous thrusts and thrust folds have the capacity to affect the location and form of hydrocarbon reserves there (Jassim and Goff 2006) [21]. More importantly, there are huge salt domes were also identified to be potential reservoirs in relation with above mentioned hydrocarbon reserves studies (Aqrawi *et al*. 2010) [4]. Moreover, in this region there are numerous amounts of ground water can be found in various layers in the Quaternary and Tertiary aquifers (Jiburi and Basrawi 2015) [2].

2.2. Data

Two distinct types of satellite images; Landsat 7 and Landsat 8 were procured from the USGS archive website (http://earthexplorer.usgs.gov/). The image is in UTM projection with zone 38 N and obtain from the United States Geological Survey (USGS), Earth Explorer website (USGS, 2017) [39]. Satellite images from the three designated years, 2002, 2012 and 2022 are used to identify ever-changing Land Use and Land Cover (LULC) pattern and environmental indicators of the study area (Fig.2 and Fig. 3). The satellite photos with the cloud percentage below 1 percent were used to undergo the ease of analysis. All Landsat images were acquired to have cloud free images that properly reflect land use features to eliminate the impact of seasonal changes and atmospheric cloud cover on image quality. The Landsat image has a spatial resolution of 30 meters by 30 meters.

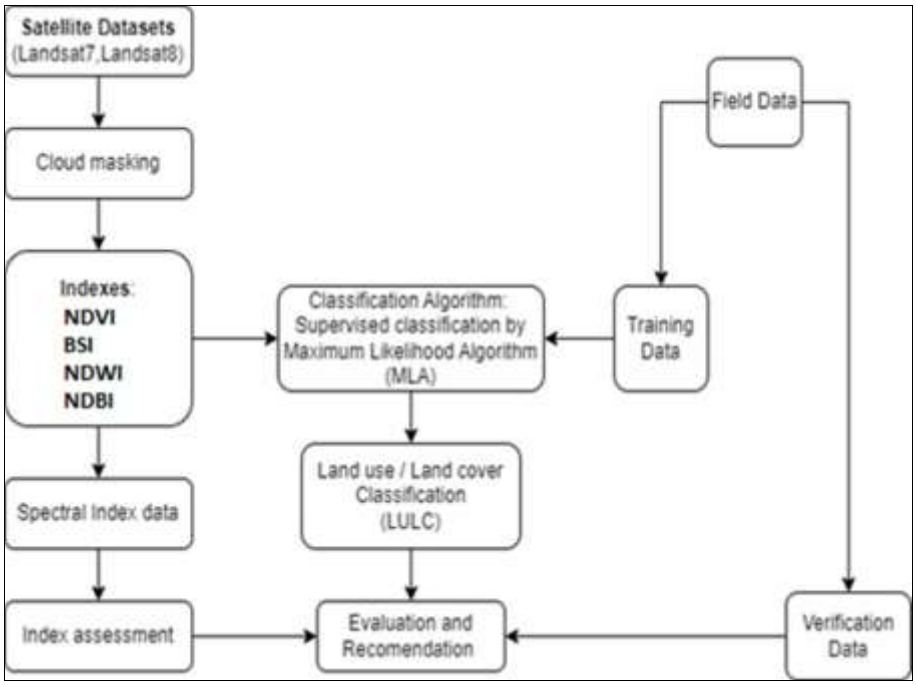

Fig 2: A flowchart for detecting changes in LULC and environmental indexes

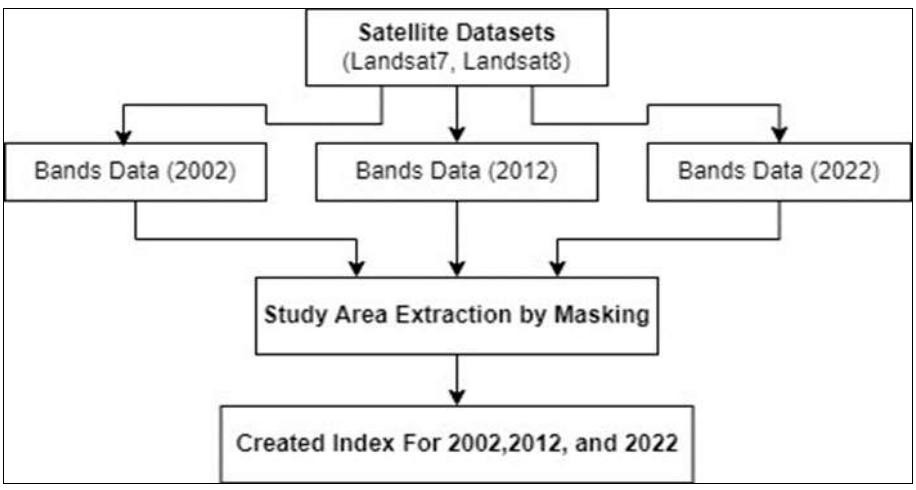

Fig 3: The calculation steps for any index used in this study

By using existing data of Basrah city, a Land Use and Land Cover (LULC) classification methodology was established. This included using Google Earth Pro, doing the GPS surveys of the site, collecting information from administrative office, interviews with local populations and stakeholders. The supervised classification was performed using Maximum Likelihood Algorithm (MLA) that employs different spectral signatures associated with each land use class. The signatures are created from specific representative samples of each training site's known Land Use and Land Cover (LULC) type.

Multiple image indices are employed to classify the picture, including but not contained too: NDVI, BSI, NDWI, and NDBI. The particular prism indices employed are presented in the table beneath.

NDVI: One of the most commonly employed remote sensing indices is the Normalized Difference Vegetation Index which measures the density and vitality of vegetation. It utilizes the near-infrared (NIR) and red (R) bands of a multispectral image, as designated by Rouse Jr. *et al*. in 1974 [32]. The Normalized Difference Vegetation Index was calculated as NDVI = (Near Infrared-Red)/(Near Infrared + Red). An NDVI's range is from -1 to 1 with greater values indicating denser and more compact vegetation (Tucker, 1979) [38]. The instance created by Pettorelli *et al*. (2005) [29] is served for crop monitoring, forest cover mapping, and land degradation analysis. NDVI is broadly employed in research corridors such as agriculture, forestry and environmental monitoring (Kerr & Ostrovsky, 2003) [22].

The index used to measure the proportion of exposed soil surfaces is the Bare Soil Index (BSI). The bare soil index (BSI) is a remote sens-ing index that emphasizes the bare soil or limited vegetation regions. The BSI is adapted from the method of Gray (1980) who used Landsat Multi-spectral Scanner (MSS) and Thematic Mapper (TM) Images respectively. They derived BSI for assessing soil erosion. The BSI is based on the assumption that bare soil reflects much more energy in the near infrared (NIR) region but a little or none in the red region. The BSI is derived from the difference of energy between the NIR and R and divided by the sum of the same energy. The BSI is written as [BSI=(NIR-R)/(NIR+R)] On the formula, R represents a red band. Higher the BSI value, the soil showed higher ratio of bare soil or sparse vegetation (Diek, 2017) [8]. Index maps Soil Erosion in China The product provides evidence for the presence of exposed land surfaces and ternary composites. Land degradation initiates desertification processes by direct soil or sand. The BSI showed the possibility of monitoring the degree of land degradation or desertification.

A remotely sensed index known as the Normalized Difference Water Index (NDWI) was employed to evaluate the water stress condition in plants by assessing variations in vegetation water content (Gao, 1996) [11]. The calculation of the NDWI is conducted using near infrared (NIR) and green (G) bands of a multispectral image. The equation describing the formula of the Normalized Difference Water Index (NDWI) is as follows:

NDWI = (Green band solution-Near Infrared band solution) / (Green band solution + Near Infrared band solution)

The value of NDWI above zero denoted so-called water pixels. NDWI assumes that vegetation is dark in the NIR domain because of the high reflectivity of water. Hence, water in the plants will be highlighted in NIR because of this low reflectivity. But the vegetation increases the amount and reflectance in the green and decrease spectral reflectance in the NIR. Since the values of reflectance is bounded by zero and one, the range of NDWI between -1 to +1.

The Normalized Difference Built-up Index is widely used for built-up areas and infrastructure detection and mapping including urban areas. It is based on the multispectral image, using the shortwave infrared and near infrared bands. There is a very simple calculation of NDBI as follows: NDBI = (SWIR-NIR) / (SWIR + NIR). High values of NDBI represent more density of built-upland. It can be used to monitor the urban expansion, land use change consequences and ecological influence of urbanization (Xu, 2008) [42].

Table 1: List of indexes involved in this study

No	Method	Formula	Reference
1.	Normalized Difference Vegetation Index (NDVI)	NDVI = (NIR-R) / (NIR + R)	Rouse *et al*., 1974 [32]
2.	Bare Soil Index (BSI)	BSI = (SWIR + R)-(NIR + B) / (SWIR + R) + (NIR + B)	Rikimaru *et al*., 2002 [31]
3.	Normalized Difference Water Index (NDWI)	NDWI = (G-NIR) / (G + NIR)	Gao, 1996 [11]
4.	Normalized Difference Built-up Index (NDBI)	NDBI = (SWIR-NIR) / (SWIR + NIR)	Zha *et al*., 2003 [43]

Information: near-infrared (NIR), red (R), green (G), blue (B), and short-wave infrared (SWIR), bands.

2.3. The LULC classes

Based on the analysis of land use, spectral responses on Landsat images, extensive field observation, and a literature review, the city of Basrah was categorized into four main classes or types of land use and land cover (LULC): water bodies, vegetation, barren land, and built-up area (Table 2). Subsequently, a supervised classification method was employed by utilizing a maximum likelihood algorithm. (Jaleta *et al*., 2016) [20] Provided a list of the LULC classes along with their corresponding descriptions.

Table 2: LULC classes and description

Land Use/Land Cover Type	Description
Vegetation	Lands occupied by crops, farmland, plantation, and fallow land.
Waterbody	Rivers, ponds, swamps, and reservoirs.
Built-up area	Infrastructures include houses, asphalt roads, buildings, and urban areas
Bare land	Lands without vegetation, crops or grasses, and barren soils.

2.4 Accuracy assessment of LULC classification

Conducting an accuracy analysis is the last stage of the research process. It is necessary to determine the level of accuracy of the investigation (Story & Congalton, 1986) [35]. Validation data is crucial in remote sensing investigations to ensure proper analysis and precise presentation of results (Lewis & Brown, 2001; Hu & Wang, 2013) [24, 18]. Evaluating the accuracy of a classified image is crucial for monitoring changes in land use and land cover (LULC) and determining the acceptability of the classification procedure. To ensure sufficient representation of all four land use and land cover (LULC) classes, 80 reference data points were selected based on their proportional area. The source of the reference ground truth data was chosen so that it should exist in the Landsat scenes of 2002, 2012 and 2022 and Google Earth map. Meanwhile, incorporating local datasets validated land use classifications. The reference data was obtained and established through visual inspections and modification (Figure 1). The accuracy assessment is the first step to assess quality and identify errors associated with input data processing. For accuracy assessment, a confusion matrix table is used, where the classification accuracy is evaluated in terms of Overall Accuracy (OA) and Kappa Statistics (K). Berberoglu & Akin (2009) [5] assert that error matrix and Kappa analysis are commonly adopted for reviewing land use change detection accuracy. The LULC classification accuracy was assessed using overall accuracy and kappa coefficient, which are calculated by investigating a "confusion matrix" or "error matrix" (Liu *et al*., 2007) [25]. Overall accuracy was computed by dividing the total number of correctly allocated pixels by the total number of referenced pixels in the matrix. (Tilahun and Teferie, 2015) [37].

A post-classification analysis was conducted for each classified Landsat image. A comparison was made for each classified Land Use and Land Cover (LULC) map from 2002 to 2012, lastly from 2012 to 2022. The software programs Arc GIS 10.8, QGIS ver. 2.8.3, Google Earth Engine, and Google Earth Pro effectively used for the evaluation and identification of the classified Landsat image.

2.5. Trends of LULC change analysis

Analyzing Land Use and Land Cover (LULC) change trend is important since it helps to identify specific land use classes or types which are undergoing transitions to other land uses (Tewabe and Fentahun, 2020) [36]. An analysis study was conducted to detect and analyze the trend of changes in land use and land cover (LULC) in Basrah city. The analysis studies compares the period from 2002 to 2012 and 2012 to 2022, which this study uses to compare the extent of each land use and land cover (LULC) class in different time periods. Land use land cover (LULC) studies provide data on the scale, scope and trajectory of land use and land cover transformations through time. The percentage and rate of changes in the study area are calculated using the number of differences between two time periods.

3. Results and Discussion

3.1. Analysis of environmental changes

Table 3 displays the NDVI findings for the study region during three specific time intervals: 2002, 2012, and 2022. The findings indicate the subsequent patterns:

The water coverage expanded from 68.48 km^2 (5.88%) in 2002 to 139.86 km^2 (12.67%) in 2012 and then remained relatively constant at 140.08 km^2 (12.03%) in 2022. In 2002, the amount of exposed soil declined from 67.61 km^2 (5.81% of the total area) to 35.14 km^2 (3.18% of the total area) in 2012. There was a small increase to 39.47 km^2 (3.39% of the total area) in 2022. The extent of sparsely vegetated land declined from 1014.23 km^2 (87.11%) in 2002 to 919.92 km^2 (83.35%) in 2012, before subsequently rising to 958.21 km^2 (82.3%) in 2022. The extent of intermediate vegetation declined from 12.94 km^2 (1.11%) in 2002 to 8.55 km^2 (0.77%) in 2012, but thereafter experienced a substantial increase to 24.92 km^2 (2.14%) in 2022. The extent of dense vegetation declined from 1.02 km^2 (0.09%) in 2002 to 0.22 km^2 (0.02%) in 2012 and thereafter rose to 1.58 km^2 (0.14%) in 2022.

Table 3: NDVI results for the study area

No.	Class	2002		2012		2022	
		Area (km^2)	Percentage	Area (km^2)	Percentage	Area (km^2)	Percentage
1	Water	68.48	5.88	139.86	12.67	140.08	12.03
2	Bare soil	67.61	5.81	35.14	3.18	39.47	3.39
3	Sparse Vegetation	1014.23	87.11	919.92	83.35	958.21	82.3
4	Moderate vegetation	12.94	1.11	8.55	0.77	24.92	2.14
5	Dense vegetation	1.02	0.09	0.22	0.02	1.58	0.14

Figure 4 illustrates a favorable trend in the study region, showing a rise in vegetation cover and water bodies, and a decline in areas of bare soil and sparse vegetation. The observed modifications indicate a general enhancement in the environmental circumstances within the research region throughout the years.

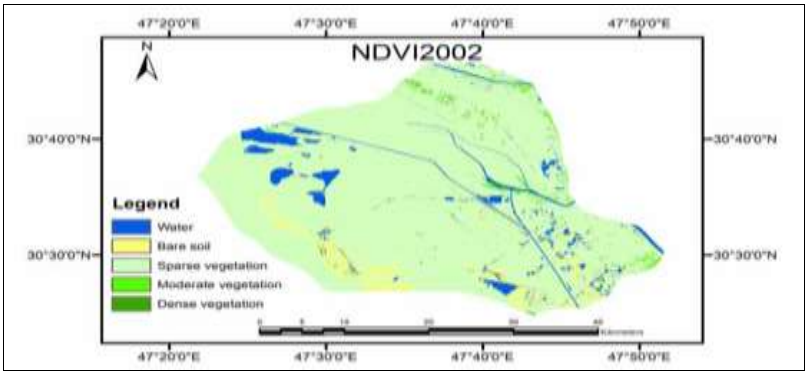

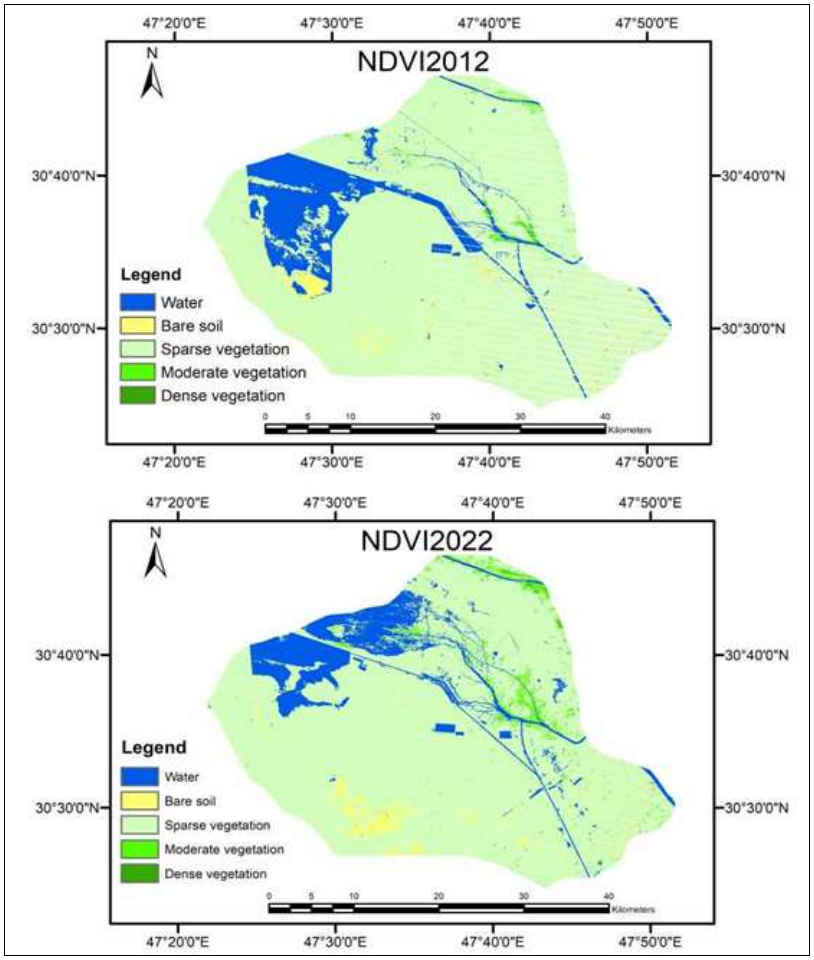

Fig 4: NDVI maps of Basrah city for the years 2002-2012-2022

Table 4 displays the area and proportion of the study area that has been classified into three distinct groups: Non-Bare Soil, Low Bare Soil, and Moderate Bare Soil. In 2002, the largest portion of the land (79.05%) was categorized as Low Bare Soil, with 20.95% classed as Non-Bare Soil, and a very small part (0.04km²) designated as Moderate Bare Soil. In 2012, there was a comparable pattern where 76.07% of the region was categorized as Low Bare Soil and 23.92% as Non-Bare Soil. The extent of Moderate Bare Soil did not change and remained at 0.04 km². Nevertheless, in the year 2022, there was a notable change in the BSI outcomes. The proportion of Non-Bare Soil area experienced a significant growth, reaching 59.66%, but the proportion of Low Bare Soil area declined to 40.33%. The extent of Moderate Bare Soil also experienced a minor rise, reaching 0.09 km².

Table 4: BSI results for the study area

No.	Class	2002		2012		2022	
		Area (km²)	Percentage	Area (km²)	Percentage	Area (km²)	Percentage
1	Non-Bare Soil	243.86	20.95	261.96	23.92	694.61	59.66
2	Low Bare Soil	920.37	79.05	833.01	76.07	469.5	40.33
3	Moderate Bare Soil	0.04	0	0.04	0	0.09	0.01

Figure 5 displays the BSI outcomes for the study region, demonstrating the spatial arrangement of various BSI categories throughout the years. By analyzing both Table 3 and Figure 4, it is possible to identify some significant patterns. The Non-Bare Soil region has shown a substantial growth from 2002 to 2022. This graph suggests a decline in the extent of exposed soil over the span of two decades. Simultaneously, the area with low bare soil has also experienced a decline from 2002 to 2022, providing more evidence of the decreasing coverage of bare soil.

On the other hand, the area of Moderate Bare Soil has remained relatively small and consistent across the years, suggesting that there has been no substantial alteration in this category over the study period. These tendencies collectively offer valuable information on the evolving soil conditions in the research area as time progresses.

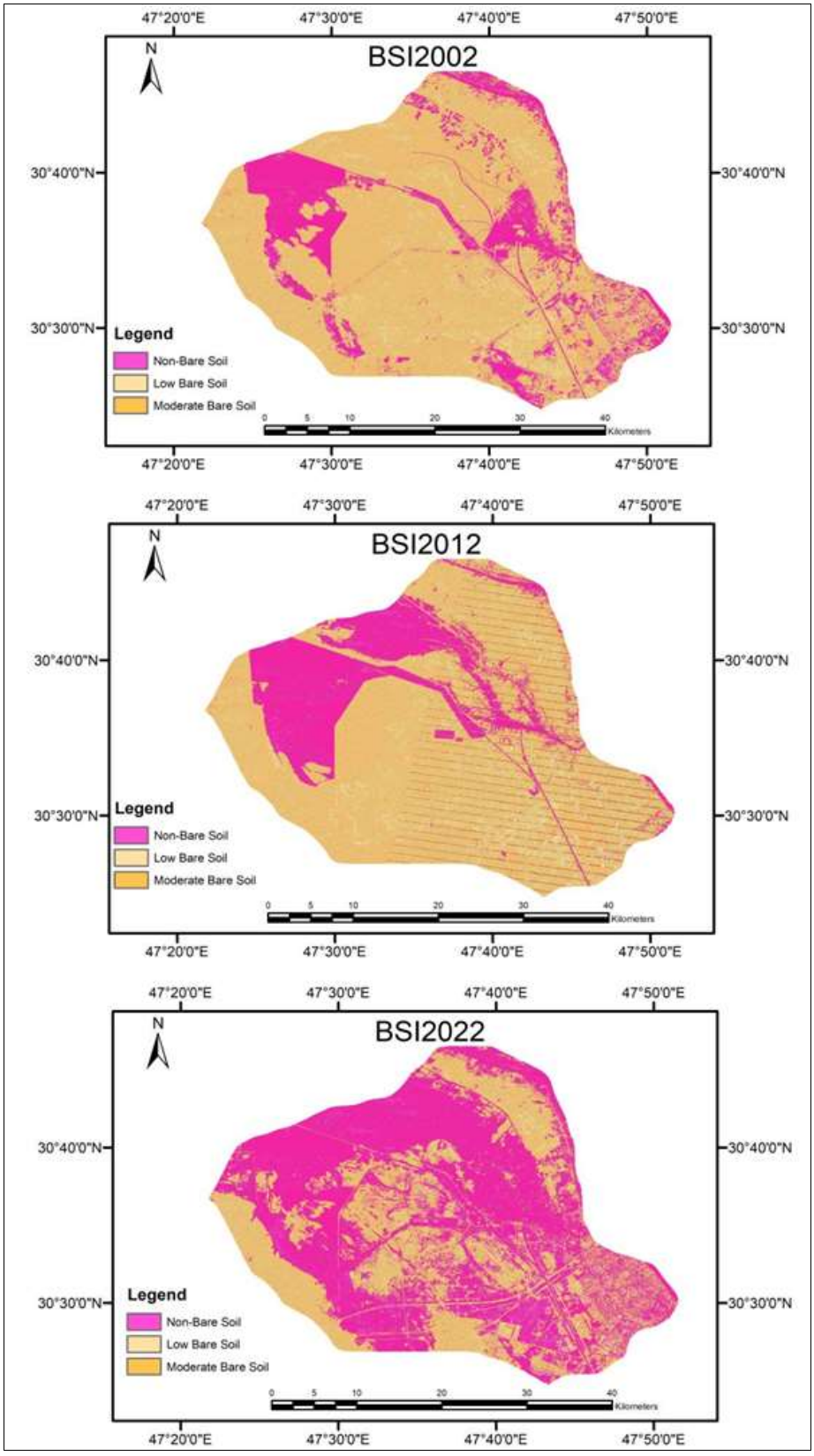

Fig 5: BSI maps of Basrah city for the years 2002-2012-2022

The NDWI findings for the research region, as depicted in Table 4.2, unveil multiple patterns. During the study period, the area affected by drought conditions gradually grew from 9.62 km^2 (0.83%) in 2002 to 10.4 km^2 (0.95%) in 2012, and then expanded further to 17.16 km^2 (1.48%) in 2022.

However, there was a notable reduction in the area affected by moderate drought conditions, with a decline from 1079.12 km^2 (92.88%) in 2002 to 937.87 km^2 (85.43%) in 2012. Subsequently, there was a modest rise to 991.4 km^2 (85.33%) in 2022, suggesting a minor revival of moderate drought conditions. The extent of the area affected by flooding or high humidity conditions originally grew from 29.2 km^2 (2.51%) in 2002 to 53.87 km^2 (4.91%) in 2012. Nevertheless, this pattern was reversed in the subsequent decade, resulting in a reduction of the area to 38.33 km^2, which accounts for a decrease of 3.3%, as of 2022.

Finally, the research period witnessed a steady growth in the water surface area. The area increased from 43.94 square kilometers (3.78% of the total) in 2002 to 95.72 square kilometers (8.72% of the total) in 2012, and then further to 114.96 square kilometers (9.89% of the total) in 2022. The data indicates a consistent increase in the size of the water surface area throughout the duration of the twenty-year research.

Table 5: NDWI results for the study area

No.	Class	2002		2012		2022	
		Area (km^2)	Percentage	Area (km^2)	Percentage	Area (km^2)	Percentage
1	Drought	9.62	0.83	10.4	0.95	17.16	1.48
2	Moderate drought	1079.12	92.88	937.87	85.43	991.4	85.33
3	Flooding, humidity	29.2	2.51	53.87	4.91	38.33	3.3
4	Water surface	43.94	3.78	95.72	8.72	114.96	9.89

The patterns reported in Table 5 for the NDWI categories align with the patterns depicted in Fig. 6. Over the years, there has been an increase in the areas affected by drought and water surface, but the area experiencing moderate drought fell from 2002 to 2012 and then saw a minor increase from 2012 to 2022. The extent of flooding experienced an initial increase in humidity from 2002 to 2012, followed by a subsequent drop from 2012 to 2022.

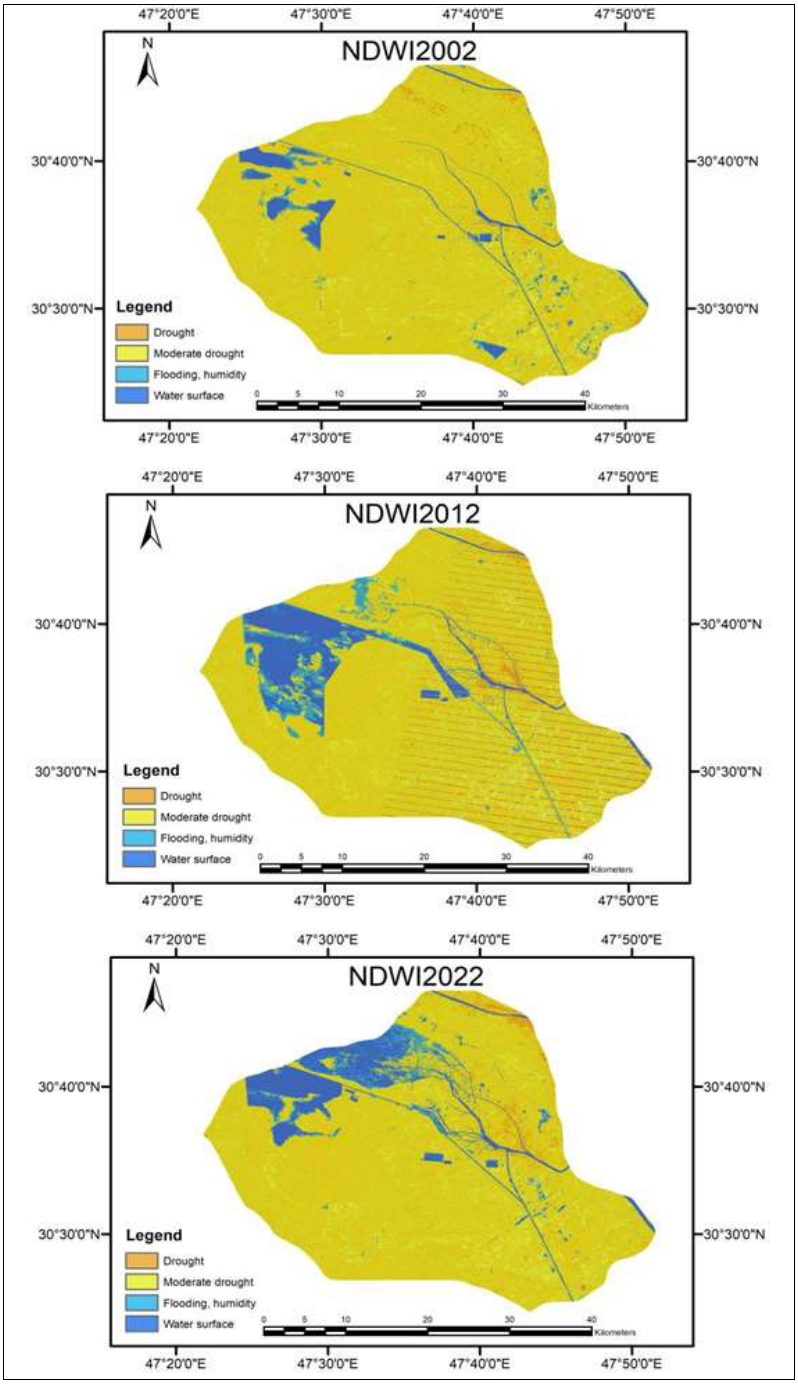

Fig 6: NDWI maps of Basrah city for the years 2002-2012-2022

Both Table 6 and Figure 7 illustrate a rise in the area of turbid water from 4.76% in 2002 to 9.66% in 2022. There is a steady rise in the amount of cloudy water observed during the 20-year timeframe. The proportion of pure water expanded from 15.09% in 2002 to 24.86% in 2022. This pattern indicates a rise in the transparency and maybe the volume of pristine water regions over a period of time. The percentage of land classified as soil, vegetation, and accumulation decreased from 80.15% in 2002 to 65.47% in 2022. This signifies a notable alteration in the utilization of land or the physical characteristics of land, resulting in a decrease in regions that are not categorized as bodies of water or developed areas. The extent of significant developed land is small, with a marginal rise from 0% in 2002 to 0.01% in 2022, suggesting a gradual but steady growth in urbanization or built-up areas.

Table 6: NDBI results for the study area

No.	Class	2002		2012		2022	
		Area (km^2)	Percentage	Area (km^2)	Percentage	Area (km^2)	Percentage
1	Turbid water	55.36	4.76	41.9	3.8	112.46	9.66
2	Clean water	175.69	15.09	255.09	23.13	289.45	24.86
3	Soil, Vegetation, Buildup	933.19	80.15	806	73.07	762.25	65.47
4	Major Built-up	0.02	0	0	0	0.1	0.01
5	Turbid water	55.36	4.76	41.9	3.8	112.46	9.66

Figure 7 exactly corresponds to the data reported in Table 6 and visually represents the changes in different land and water categories during the same timeframes. The data emphasizes the changes in murky water, clear water, soil/vegetation accumulation, and significant urbanized regions. An evident decline in the soil, vegetation, and developed area indicates a change in land cover, maybe caused by a rise in water bodies or alterations in land utilization. However, the small rise in large developed regions suggests that urban growth has not had a substantial role in the research area over the observed timeframe.

This image provides a graphical representation of the NDBI findings for the research area, highlighting important patterns. The area of water with high levels of suspended particles, indicated by the color red, had a substantial rise between 2012 and 2022. The region designated for clean water, indicated by the color blue, consistently expanded throughout the course of 20 years. Conversely, the soil, vegetation, and built-up area, depicted in green, diminished with time. Finally, the predominant developed region, depicted in purple, remained relatively modest over the whole duration, so emphasizing that urban growth did not significantly contribute to the alterations in the studied area.

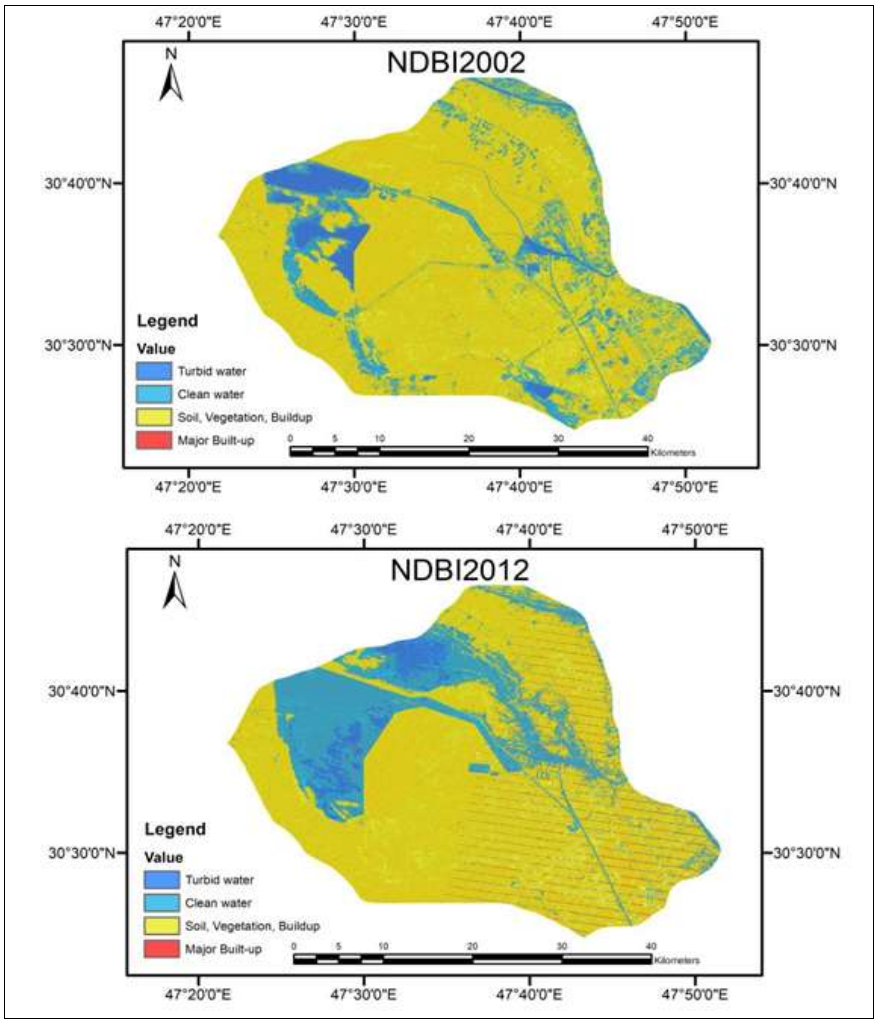

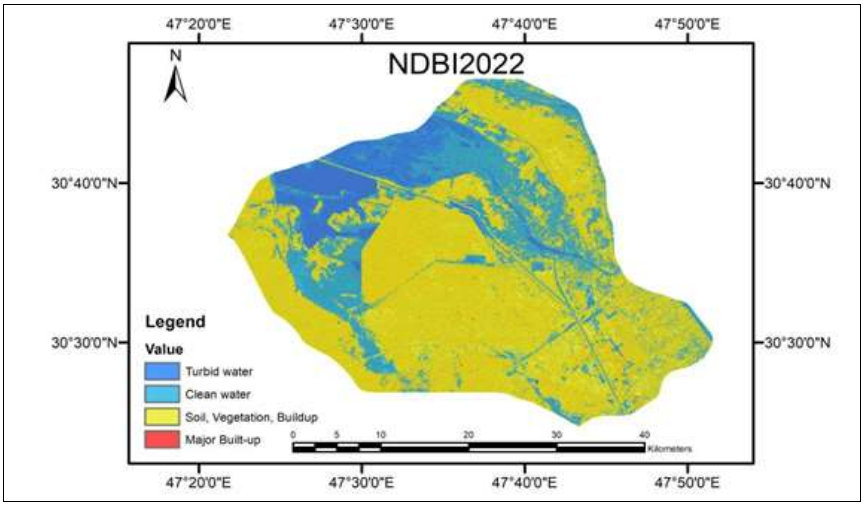

Fig 7: NDBI maps of Basrah city for the years 2002-2012-2022

Figure 9 presents a graphical depiction of the NDBI findings for the research region, providing a spatial view of the distribution of several NDBI categories. The visual representation is crucial for comprehending the geographic distribution and density of these classes throughout the study area.

An important tendency to note is the rise in both locations with cloudy and clear water. The diagram illustrates the growth of these regions throughout time, serving as a visual validation of the information contained in Table 6. This trend may suggest alterations in the quality and amount of water, or both, and could be a manifestation of shifts in environmental conditions, such as variations in precipitation patterns or modifications in land use.

In contrast, the image also demonstrates a decline in the areas categorized as soil, vegetation, and built-up land. The decrease in size of these areas over the research period is clearly shown in Figure 9. This phenomenon can be attributed to a multitude of variables, encompassing natural processes such as erosion, as well as human activity like urbanization and deforestation.

3.2 Analysis of LULC classification

During the classification of Landsat images (2002, 2012, and 2022), four main land use and land cover (LULC) types were considered in the study region: Waterbody, Vegetation, Bare land, and Built-up area (Fig. 8). Table 7 presents the area coverage in kilometer squares (km^2) and percentage (%) of each land use and land cover (LULC) class in Basrah city for the three time periods (2002, 2012, and 2022). Figure 9 displays the extent of land use and land cover (LULC) for each class during the study periods. Table 7 displays the alterations in land use and land cover (LULC) in Basrah city between 2002 and 2022. The table demonstrates a substantial rise in the area covered by water bodies, which grew from 65.75 km² (5.66%) in 2002 to 154.59 km² (13.31%) in 2022. This indicates a growth of 88.84 km² (7.65%) during the span of 20 years, as presented in Table 7. This phenomenon aligns with prior research that has documented the enlargement of aquatic ecosystems in urban regions as a result of human endeavors such as construction and infrastructure advancement.

In contrast, the region experienced a sharp drop in vegetation coverage. It plummeted from 234.78 km² (20.21%) in 2002 to 32.43 km² (2.79%) in 2022, which means that there was a huge drop of 202.35 km² (17.42%) in the same period (Table 7). The decline is worrisome since plants have a critical role in conserving ecosystem services and reducing the intensity of urban heat island effect (Bolund & Hunhammar, 1999) [6].

Notable changes in the extent of barren land and developed areas, indicated in Table7, can be observed (Table 7). The area of barren land decreased from 780.59 km² (67.18%) in 2002 to 750.18 km² (64.57%) in 2022. The built-up areas increased from 80.77 km² (6.95%) in 2002 to 224.63 km² (19.33%) in 2022. These adjustments imply that urbanization and human activities have resulted in changes from natural habitats to developed areas, leading to habitat fragmentation and the decline of biodiversity (Hannah *et al.*, 1995) [15].

Table 7: The area coverage in kilometer squares (km^2) and percentage (%) of LULC classes in Basrah city

LULC Category	2002		2012		2022	
	Area (km^2)	Area (%)	Area (km^2)	Area (%)	Area (km^2)	Area (%)
Water body	65.75	5.66	183.33	15.78	154.59	13.31
Vegetation	234.78	20.21	125.49	10.8	32.43	2.79
Barren land	780.59	67.18	684.45	58.91	750.18	64.57
Built-up area	80.77	6.95	168.58	14.51	224.63	19.33
TOTAL	1161.85	100	1161.85	100	1161.85	100

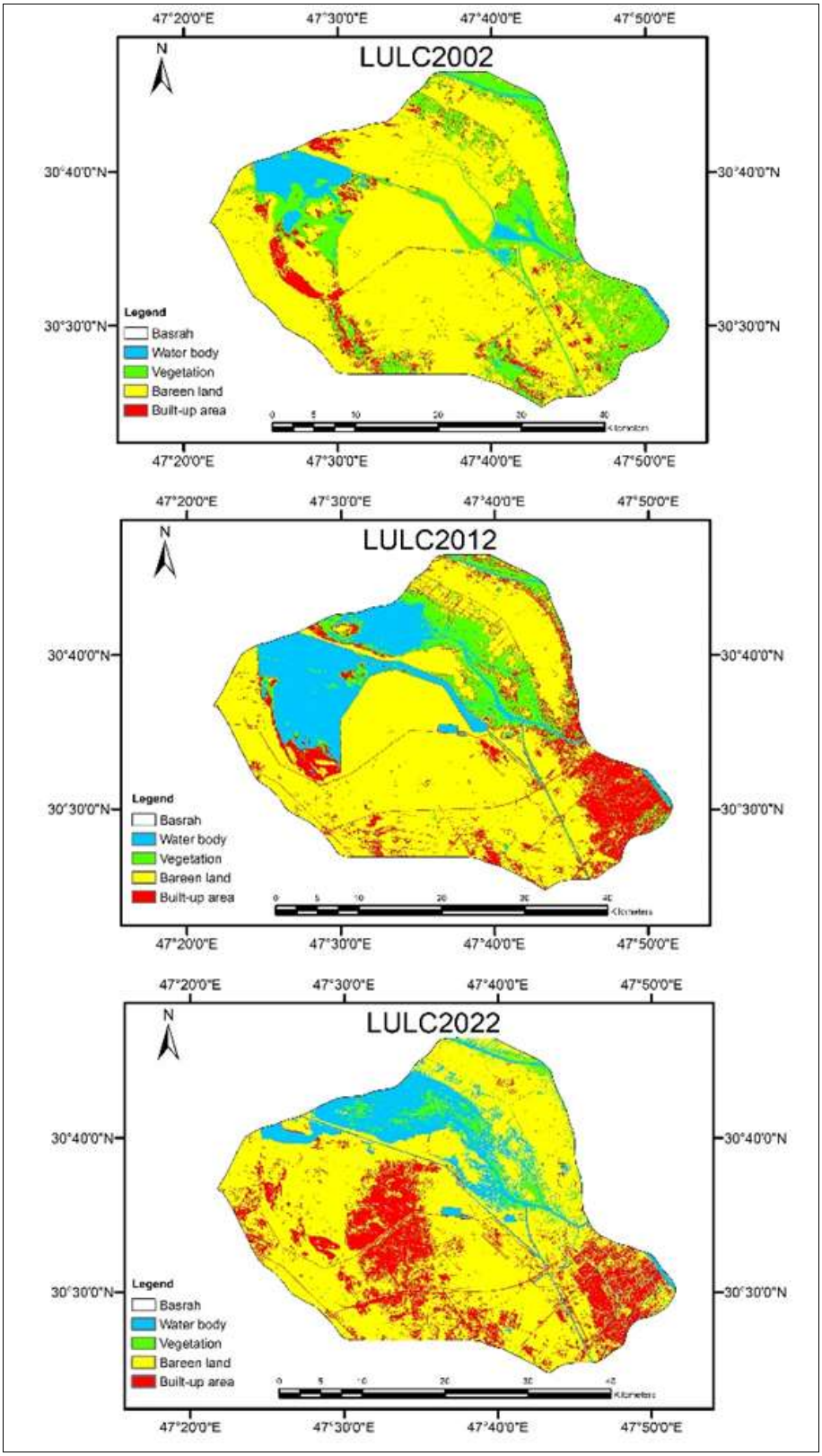

Fig 8: Land use / Land cover maps (2002-2022)

Table 8 and Figure 10 display the land use and land cover (LULC) changes in Basrah city on 2002 till 2022. This table and figure in this paper show the changes in land use and land cover (LULC) in Basrah city from 2002 till 2022. In the table, there has been a significant shift in land use and land cover (LULC) classes over the two decades. The area covered by water bodies experienced a notable increase of 88.84 km² (7.65%) between 2002 and 2022. This increase was mostly driven by a considerable growth of 117.58 km² (10.12%) from 2002 to 2012. However, there was a subsequent reduction of 28.74 km² (-2.47%) from 2012 to 2022.

On the other hand, the amount of vegetation in the region declined by 202.35 km² (-17.42%) from 2002 to 2022. This reduction consisted of a decrease of 109.29 km² (-9.41%) from 2002 to 2012, followed by a further decrease of 93.06 km² (-8.01%) from 2012 to 2022, as seen in table 7. The observed pattern aligns with prior research indicating a

decrease in vegetation density in urban regions as a result of urbanization and human actions.

The extent of barren land dropped by 30.41 km² (-2.61%) from 2002 to 2022, with a decline of 96.14 km² (-8.27%) from 2002 to 2012. However, there was an increase of 65.73 km² (5.66%) from 2012 to 2022, as shown in Table 7. This pattern aligns with the results of other studies that have documented a decline in unproductive land as a result of urbanization and changes in land use (Li *et al*., 2019).

Moreover, the total land area occupied by developed areas grew by 143.86 km² (12.38%) between 2002 and 2022. This growth consisted of an increase of 87.81 km² (7.56%) from 2002 to 2012, followed by an additional increase of 56.05 km² (4.82%) from 2012 to 2022 (Table 7). The pattern is consistent with previous research which showed that, as cities grew and the populations expanded.

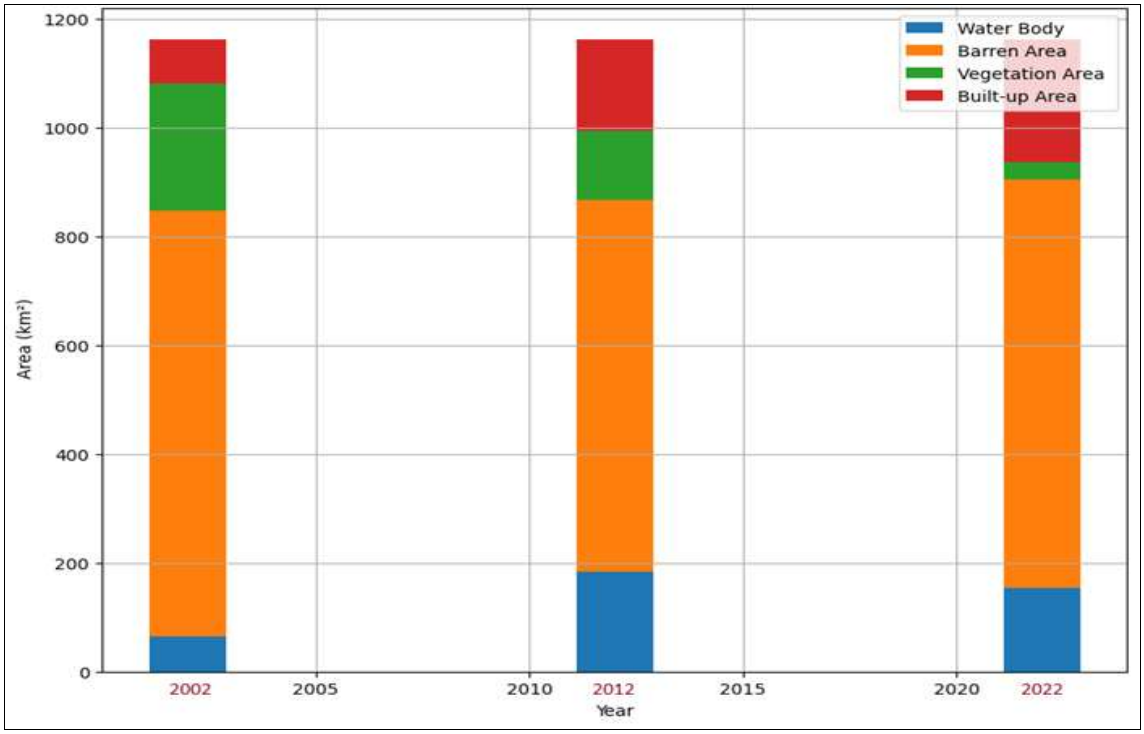

Fig 9: Area of LULC classes (2002-2022)

Accuracy of the classification was assessed using the LULC maps from 2002, 2012, and 2022. The overall accuracy of the 2002, 2012, and 2022 LULC maps were 93.75%, 100%, and 94.73% respectively. The kappa coefficients for these maps were 0.91, 1.00, and 0.93 respectively. Therefore, these findings suggest that the classified map and the actual land use and land cover (LULC) classes exhibited agreement. The classified map also identified the minimum level of accuracy that is necessary for the post-classification activities as will be discussed in the following sub-section.

Table 8: LULC change analysis in 10 years' interval from 2002 to 2022.

LULC Category	2002-2012		2012-2022		2002-2022	
	Area (km²)	Change (%)	Area (km²)	Change (%)	Area (km²)	Change (%)
Water body	117.58	10.12	-28.74	-2.47	88.84	7.65
Vegetation	-109.29	-9.41	-93.06	-8.01	-202.35	-17.42
Barren land	-96.14	-8.27	65.73	5.66	-30.41	-2.61
Built-up area	87.81	7.56	56.05	4.82	143.86	12.38

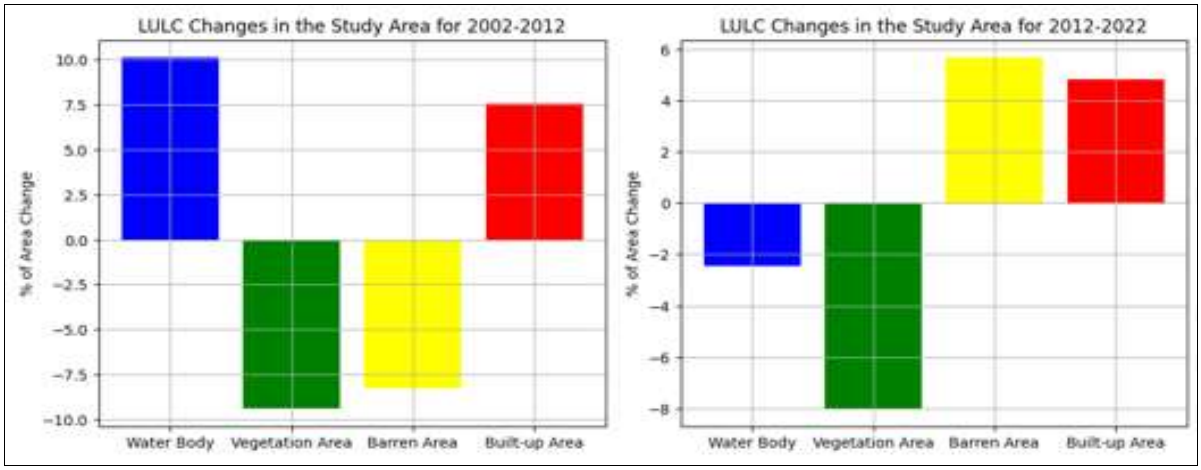

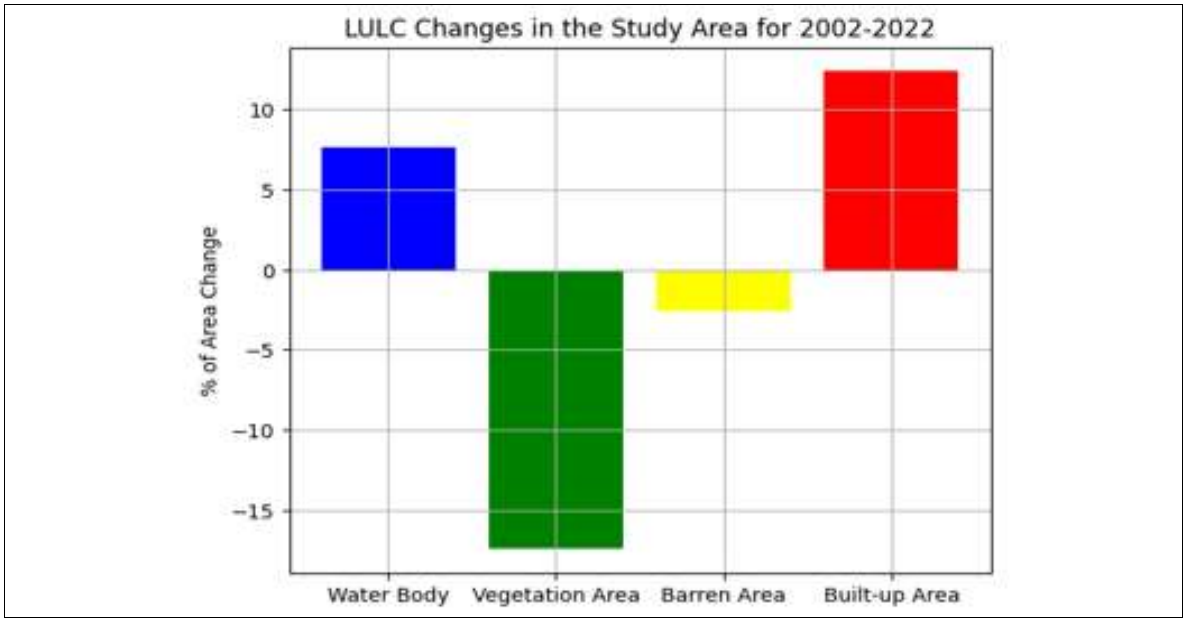

Fig 10: Rate of class's area change for the study area

4. Conclusion

This study aims to utilize geospatial technology to examine the dynamics of Land Use Land Cover (LULC) in Basrah province for the last 20 years (2002-2022). These changes were investigated by applying satellite images for (2002, 2012, 2022). Only Landsat images with less than 1% cloud cover were used in the study area to enable the study to be done. To avoid the seasonal variations effect and the effect of atmosphere cloud cover which causes in degradation of the image quality, this requires obtaining the images used to be cloud free and to represents the land cover feature object of interest correctly. During the 20 years between 2002 and 2022, Basrah city had many changes in Land Use and Land Cover (LULC). The extent of water bodies had a significant increase, rising from 65.75 km² (5.66%) in 2002 to 154.59 km² (13.31%) in 2022, indicating a major growth in the area covered by water bodies. Conversely, there was a substantial decline in the extent of vegetation, dropping from 234.78 km² (20.21%) in 2002 to 32.43 km² (2.79%) in 2022, signifying a noteworthy depletion of vegetation during the same timeframe. The amount of land that was unproductive demonstrated a modest decrease from 780.59 sq. km^2 (67.18%) in 2002 to 750.18 sq. km^2 (64.57%) in 2022. What significantly increased is the urbanization as the urban areas multiplied, it increased from 80.77 $sq.km^2$ (6.95%) in 2002 to 224.63 sq. km (19.33%) in 2022.

The present research has shown that the recorded transformations in Land Use and Land Cover (LULC) are largely the outcome of the swelling populace and the subsequent demand of natural resources which ultimately caused deforestation for different purposes in the city of Basrah. Definitely, these changes of LULC prompted a number of negative consequences on our planet Earth, for example, land degradation and erosions, declining biodiversity, destructions of ecosystem services and disturbance of hydrologicals cycle.

The research domain shows a worrying deficit of arable cultivable acres due to the conversion rate of bushland, grassland, woodland, and steep slopes for agricultural purposes for crop cultivation, hence resulting in significant levels of land degradation and soil erosion. Moreover, the cultivation of lands that are marginal and of steep slope, without drawing an appropriate soil management plan, lead to significant levels of soil degradation, and in case of a heavy rainfall or flood, the runoff of soil will affect the local stream; thereafter, simply because of the siltation of the stream, it would not be lucrative for fisheries.

Many people living in poverty depend on the sale of firewood, charcoal, and construction materials as their main income-producing activities. Consequently, the application sustainable integrated watershed management approaches are crucial.

The findings demonstrate the in-scope area hugely demand sustainable LULC approaches such as integrated watershed management for conserving and utilizing the NMSs wisely in the future recommended that the locals, stakeholders, politicians, governmental and non-governmental organizations has to have roles in enhancing awareness.

5. References

1. Ahmed A, Al-Saady YI, Al-Khafaji AK, Gloaguen R. Environmental change detection in the central part of Iraq using remote sensing data and GIS. Iraqi Journal of Science. 2014;7(3).
2. Al-Jiburi HK, Al-Basrawi NH. Hydrogeological map of Iraq, scale 1:1000 000, 2013. Iraqi Bulletin of Geology and Mining. 2015;11(1):17-26.
3. Angelsen A, Kaimowitz D, eds. Agricultural Technologies and Tropical Deforestation. CAB International; c2001.
4. Aqrawi AA, Goff JC, Horbury AD, Sadooni FN. The Petroleum Geology of Iraq (Vol. 424). Beaconsfield: Scientific Press; c2010.
5. Berberoglu S, Akın A. Assessing different remote sensing techniques to detect land use/cover changes in the eastern Mediterranean. Turkish Journal of Agriculture and Forestry. 2009;11(1):46-53.
6. Bolund P, Hunhammar S, Hunhammar S. Ecosystem

services in urban areas. Ecological Economics. 1999;29(2):293-301.
7. Chen X, Zhao HM, Li P, Yin ZY. Remote sensing image-based analysis of the relationship between urban heat island and land use/cover changes. International Journal of Remote Sensing. 2006;104(2):133-146.
8. Diek S, Fornallaz F, Schaepman ME, De Jong R. Barest pixel composite for agricultural areas using Landsat time series. Remote Sensing. 2017;9(12):1245.
9. Fearnside PM. Deforestation in Brazilian Amazonia: history, rates, and consequences. Conservation Biology. 2005;19(3):680-688.
10. Foley JA, DeFries R, Asner GP, *et al*. Global consequences of land use. Science. 2005;309(5734):570-574.
11. Gao BC. NDWI-A normalized difference water index for remote sensing of vegetation liquid water from space. Remote Sensing of Environment. 1996;58(3):257-266.
12. Gao Q, Zribi M, Escorihuela MJ, Baghdadi N. Synergetic use of Sentinel-1 and Sentinel-2 data for soil moisture mapping at 100 m resolution. Sensors. 2017;17(9):1966.
13. Geist HJ, Lambin EF. Proximate causes and underlying driving forces of tropical deforestation: Tropical forests are disappearing as the result of many pressures, both local and regional, acting in various combinations in different geographical locations. BioScience. 2002;52(2):143-150.
14. Hadeel AS, Jabbar MT, Chen X. Remote sensing and GIS application in the detection of environmental degradation indicators. Journal of Environmental Management. 2011;14(1):39-47.
15. Hannah L, Carr JL, Lankerani A. Human disturbance and natural habitat: a biome level analysis of a global data set. Biodiversity and Conservation. 1995;4(2):128-155.
16. He C, Shi P, Xie D, Zhao Y. Improving the normalized difference built-up index to map urban built-up areas using a semiautomatic segmentation approach. Remote Sensing Letters. 2010;1(4):213-221.
17. Houghton RA. Revised estimates of the annual net flux of carbon to the atmosphere from changes in land use and land management 1850-2000. Tellus B: Chemical and Physical Meteorology. 2003;55(2):378-390.
18. Hu S, Wang L. Automated urban land-use classification with remote sensing. International Journal of Remote Sensing. 2013;34(3):790-803.
19. Huang J, Wang H, Dai Q, Han D. Analysis of NDVI data for crop identification and yield estimation. IEEE Journal of Selected Topics in Applied Earth Observations and Remote Sensing. 2014;7(11):4374-4384.
20. Jaleta D, Mbilinyi B, Mahoo HF, Lemenih M. Evaluation of Land Use/Land Cover Changes and Eucalyptus Expansion in Meja Watershed, Ethiopia. Ethiopian Journal of Environmental Studies & Management. 2016;7(3):1-2.
21. Jassim SZ, Goff JC. Eds. Geology of Iraq. DOLIN, SRO; c2006.
22. Kerr JT, Ostrovsky M. From space to species: ecological applications for remote sensing. Trends in Ecology & Evolution. 2003;18(6):299-305.
23. Lambin EF, Turner BL, Geist HJ, *et al*. The causes of land-use and land-cover change: moving beyond the myths. Global Environmental Change. 2001;11(4):261-269.
24. Lewis HG, Brown M. A generalized confusion matrix for assessing area estimates from remotely sensed data. International Journal of Remote Sensing. 2001;22(16):3045-3050.
25. Liu C, Frazier P, Kumar L. Comparative assessment of the measures of thematic classification accuracy. International Journal of Remote Sensing. 2007;28(4):847-854.
26. McFeeters SK. The use of the Normalized Difference Water Index (NDWI) in the delineation of open water features. International Journal of Remote Sensing. 1996;17(7):1425-1432.
27. Nguyen CT, Chidthaisong A, Kieu Diem P, Huo LZ. A modified bare soil index to identify bare land features during agricultural fallow-period in Southeast Asia using Landsat 8. Land. 2021;10(3):231.
28. Nugroho JT. Identification of Inundated Area Using Normalized Difference Water Index (NDWI) on lowland region of Java Island. International Journal of Remote Sensing and Earth Sciences (IJReSES). 2013;10(2):59-70.
29. Pettorelli N, Vik JO, Mysterud A, Gaillard JM, Tucker CJ, Stenseth NC. Using the satellite-derived NDVI to assess ecological responses to environmental change. Trends in Ecology & Evolution. 2005;20(9):503-510.
30. Pielke Sr RA, Pitman A, Niyogi D, Mahmood R, McAlpine C, Hossain F, *et al*. Land use/land cover changes and climate: Modeling analysis and observational evidence. Wiley Interdisciplinary Reviews: Climate Change. 2011;2(6):828-850.
31. Rikimaru A, Roy PS, Miyatake S. Tropical forest cover density mapping. Tropical Ecology. 2002;43(1):39-47.
32. Rouse JW, Haas RH, Schell JA, Deering DW. Monitoring vegetation systems in the Great Plains with ERTS. NASA Spec. Publ. 1974;351(1):309.
33. Schmidhuber J, Tubiello FN. Global food security under climate change. Proceedings of the National Academy of Sciences. 2007;104(50):19703-19708.
34. Seto KC, Reenberg A, Boone CG, Fragkias M, Haase D, Langanke T, *et al*. Urban land teleconnections and sustainability. Proceedings of the National Academy of Sciences. 2012;109(20):7687-7692.
35. Story M, Congalton RG. Accuracy assessment: a user's perspective. 1986;52(3):397-414.
36. Tewabe D, Fentahun T. Assessing land use and land cover change detection using remote sensing in the Lake Tana Basin, Northwest Ethiopia. 2020;6(1):15-27.
37. Tilahun A, Teferie B. Accuracy Assessment of Land Use Land Cover Classification using Google Earth. 2015;4(4):1-10.
38. Tucker CJ. Red and photographic infrared linear combinations for monitoring vegetation. Remote Sensing of Environment. 1979;8(2):127-150.
39. US Geological Survey. Landsat Data; USGS: Reston, VA, USA; c2017.
40. Wu C, Niu Z, Tang Q, Huang W. Estimating chlorophyll content from hyperspectral vegetation indices: Modeling and validation. Agricultural and Forest Meteorology. 2008;148(8-9):1230-1241.
41. Xu H. Modification of normalised difference water index (NDWI) to enhance open water features in

remotely sensed imagery. International Journal of Remote Sensing. 2006;27(14):3025-3033.
42. Xu H. A new index for delineating built-up land features in satellite imagery. 2008;29(14):3635-3653.
43. Zha Y, Gao J, Ni S. Use of normalized difference built-up index in automatically mapping urban areas from TM imagery. International Journal of Remote Sensing. 2003;24(3):583-594.
44. Zhu XM, Song XN, Leng P, Guo D, Cai SH. Impact of atmospheric correction on spatial heterogeneity relations between land surface temperature and biophysical compositions. IEEE Transactions on Geoscience and Remote Sensing. 2021;59(3):2680-2697.
45. Li J, Zou B, Yeo YH, Feng Y, Xie X, Lee DH, *et al*. Prevalence, incidence, and outcome of non-alcoholic fatty liver disease in Asia, 1999-2019: A systematic review and meta-analysis. The Lancet Gastroenterology & Hepatology. 2019 May;4(5):389-398.